A Climatology of the Extratropical Transition of Atlantic Tropical Cyclones

ROBERT E. HART AND JENNI L. EVANS

Department of Meteorology, The Pennsylvania State University, University Park, Pennsylvania

(Manuscript received 16 June 1999, in final form 1 April 2000)

ABSTRACT

A comprehensive climatology of extratropically transitioning tropical cyclones in the Atlantic basin is presented. Storm tracks and intensities over a period from 1899 to 1996 are examined. More detailed statistics are presented only for the most reliable period of record, beginning in 1950.

Since 1950, 46% of Atlantic tropical cyclones transitioned to the extratropical phase. The coastal Atlantic areas most likely to be impacted by a transitioning tropical cyclone are the northeast United States and the Canadian Maritimes (1–2 storms per year), and western Europe (once every 1–2 yr). Extratropically transitioning tropical cyclones represent 50% of landfalling tropical cyclones on the east coasts of the United States and Canada, and the west coast of Europe, combined. The likelihood that a tropical cyclone will transition increases toward the second half of the tropical season, with October having the highest probability (50%) of transition.

Atlantic transition occurs from 24° to 55°N, with a much higher frequency between the latitudes of 35° and 45°N. Transition occurs at lower latitudes at the beginning and end of the season, and at higher latitudes during the season peak (August–September). This seasonal cycle of transition location is the result of competing factors. The delayed warming of the Atlantic Ocean forces the location of transition northward late in the season, since the critical threshold for tropical development is pushed northward. Conversely, the climatologically favored region for baroclinic development expands southward late in the season, pinching off the oceanic surface area over which tropical development can occur. The relative positions of these two areas define the typical life cycle of a transitioning tropical cyclone: tropical intensification, tropical decay, extratropical transition and intensification, occlusion.

Using a synthesis of National Hurricane Center Best-Track data and European Centre for Medium-Range Weather Forecasts reanalyses data, the intensity changes during and after transition are evaluated. It is extremely rare for a transitioning tropical cyclone to regain (in the extratropical phase) its peak (tropical phase) intensity. However, of the 61 transitioning tropical storms during the period 1979–93, 51% underwent post-transition intensification. Over 60% of cyclones that underwent post-transition intensification originated south of 20°N. In contrast, 90% of tropical cyclones that underwent post-transition decay originated north of 20°N. This suggests that strong baroclinic characteristics during formation are not necessary for strong post-transition development; in fact, they appear to hinder post-transition intensification and, therefore, the post-transition life span of the cyclone itself.

1. Introduction

Tropical cyclones and extratropical cyclones have been studied separately for nearly a century. The advent of satellites has heightened our awareness that cyclones of one type can transition into cyclones of the other. Such transitions typically represent departures from the conventional methods for cyclone development. For tropical cyclones, this most often occurs when the storm moves over colder water and into stronger shear at higher latitudes, and is referred to as extratropical transition. During the past century, numerous memorable cases of transition have occurred, including the New England Hurricane of 1938 (Pierce 1939), Hazel [(1954); Palmén 1958], Agnes (1972), The Unnamed Storm (1991), Fran (1996), Luis (1996), Danny (1997), and Floyd (1999).

Previous research on Atlantic transitions has been almost exclusively through case studies. Palmén (1958) found that overall potential energy of the atmosphere increased during the transformation of Hazel (1954), since the energy from latent heat release exceeded the release of kinetic energy. This would suggest that transforming tropical storms produce, at least temporarily, an environment that is more conducive to baroclinic growth following transition than was the case prior to transition. In the 1950s, Sekioka (1956a,b; 1957) found that the process of west Pacific transition was essentially the transient superposition of two cyclones: the decaying hurricane vortex and the growing extratropical cyclone. By subtracting the estimated symmetric pressure perturbation associated with the tropical vortex, the evolving extratropical cyclone could be analyzed. Matano and

Corresponding author address: Mr. Robert E. Hart, Department of Meteorology, The Pennsylvania State University, 503 Walker Building, University Park, PA 16802-5013.
E-mail: hart@ems.psu.edu

Sekioka (1971) presented the first classification system for the transition process: complex and compound transitions. Further synoptic analyses of transition were performed by Kornegay and Vincent (1976), DiMego and Bosart (1982a,b), Bosart and Bartlo (1991), Bosart and Lackmann (1995). These analyses showed that the transition process was far more complicated than the superposition scenario proposed by Sekioka. Further, once a larger observational database was examined, the surface pressure–based classification system presented by Matano and Sekioka was found to be too simplistic to adequately describe transition in the Pacific Ocean (Klein 1997).

While recent research has made advances in the area of transition, the scientific community still does not have an adequate understanding of the geographic and temporal distribution of transition in the Atlantic basin (Malmquist 1999). To fill this need, a comprehensive climatology of extratropical transition in the Atlantic basin is presented here. A similar climatology has been performed for the Pacific basin (Brand and Guard 1978; Klein 1997).

This paper presents the Atlantic transition problem from a large-scale, climatological perspective. Ongoing work by the authors is underway to examine the mesoscale and synoptic-scale aspects of North Atlantic transition. The methodology is presented in section 2, results are given in sections 3–7, a summary is given in section 8, and conclusions in section 9.

2. Methodology

The climatology uses a combination of datasets spanning variable periods over the past 97 yr. Definitions for key terms are given below, along with descriptions and analysis methodology of each dataset.

a. Definitions

At the current time, there is no objective definition for transition that is widely accepted by the meteorological community (Malmquist 1999). For the purposes of this study, the definition of extratropical transition will be the declaration of transition given by the National Hurricane Center (NHC) in the best-track dataset (Neumann et al. 1993; Jarvinen et al. 1984). This declaration of transition is arrived at through subjective examination by NHC of two factors: underlying sea surface temperature (SST) and subjective satellite interpretation of storm structure and asymmetry (L. Avila 1999, personal communication). Consequently, there is considerable uncertainty in the accuracy of the point at which a tropical system begins to lose its tropical characteristics. The NHC declaration typically occurs early in the 1–2-day period of transition, when the storm is just beginning to lose its tropical characteristics.

In this study, ''transitioning tropical cyclone'' is defined as a storm that transitions from tropical to extratropical at some point in its lifetime. The tropical phase refers to the period of the storm's life cycle prior to the NHC transition point. Extratropical (ET) phase refers to the period of the storm's lifecycle after the NHC transition point. A direct hit by a tropical cyclone is defined here as the center of the cyclone passing within 60 nmi (111 km) of a given location. This 60-nmi distance is consistent with the displacement used by NHC to define strike probabilities during the hurricane season for any existing tropical cyclone. This is also a typical radius for damaging winds in a tropical cyclone.

Minimum sea level pressure is used for measuring the cyclone's intensity, both prior to and following transition. Post-transition intensity change is then defined as a comparison of the minimum sea level pressure at the last tropical cyclone report (as a tropical system) in the best-track dataset to the minimum sea level pressure thereafter in the cyclone's life span.

b. Datasets and their analysis

The NHC best-track dataset (Neumann et al. 1993; Jarvinen et al. 1984) is used as the primary source of tracks and intensities for Atlantic tropical cyclones from 1899 to 1996. This dataset provides positions and intensities (estimated maximum wind and minimum pressure) at 6-h intervals for every Atlantic tropical cyclone since 1886. Landsea (1993) found that the accuracy of the best-track data prior to 1944 was questionable given minimal direct observations of pressure or wind. Consequently, detailed analyses of this transition climatology are limited to the post-1950 period, for which reconnaissance measurements of pressure and wind, and satellite-based estimates of intensity, are available. However, problems remain with the best-track dataset in the post-1950 era. Aircraft reconnaissance flights into storms typically stop once the storm is no longer a threat to land, or the storm passes north of 40°N. This results in an incomplete set of best-track data for tropical cyclones that have begun to transition. Many storm tracks in the best-track database are halted at the transition point or soon after (see Table 1). Therefore, making post-transition pressure change diagnostics based solely upon the NHC best-track dataset is problematic and can be biased toward transitions near land and in lower latitudes.

To fill in gaps in the database of post-transition pressure change statistics, the European Centre for Medium-Range Weather Forecasts (ECMWF) 2.5° resolution reanalysis fields spanning the period 1979–93 are used (Gibson et al. 1997). In addition to the conventional surface and upper-air observations, satellite-derived temperature and moisture perturbations are incorporated into these analyses. Thus, the ECMWF reanalyses grossly capture synoptic and (occasionally) coarse mesoscale (meso-α) phenomena over the oceans where conventional surface and upper-air data are scant. While the coarse resolution of the analyses limit the detail resolved, gross tropical cyclone structure can indeed be

TABLE 1. Summary of the 61 tropical cyclones that transitioned during the ECMWF reanalyses dataset period, 1979–93. The date and location of transition point as defined by NHC are given, followed by the number of 6-hourly NHC advisories issued during the extratropical phase. Note that for 38 of the 61 storms (62%), at most two reports were issued for the extratropical phase. The seventh and eighth columns specify the intensity of the cyclone from the last NHC tropical report. The last two columns give the intensity change of the cyclone (as measured by central pressure change in hPa, ΔP) after the last tropical advisory. NHC ΔP is the maximum intensity change using NHC advisories, if at least three were available (N/A given otherwise). REAN ΔP is the maximum intensity change using the ECMWF reanalyses. If the cyclone never regains the pretransition intensity (weakens, denoted by "+" in table), no magnitude is given.

Year	Name	Transition date	Transition latitude	Transition longitude	No. ET reports	Last tropical wind (kt)	Last tropical pressure (hPa)	NHC ΔP (hPa)	REAN ΔP (hPa)
1979	David	06 Sep	43.3	−73.7	6	40	991	−6	−12
1979	Frederic	14 Sep	42.5	−76.0	2	35	997	−9	−20
1979	Gloria	15 Sep	45.0	−32.0	1	65	992	N/A	+
1979	Henri	24 Sep	26.4	−86.7	1	20	1011	N/A	+
1980	Bonnie	19 Aug	51.0	−36.0	1	65	995	N/A	+
1980	Earl	10 Sep	49.5	−28.5	2	55	N/A	N/A	−30
1980	Francos	21 Sep	54.0	−29.0	1	50	998	N/A	N/A
1980	Ivan	12 Oct	52.5	−24.5	1	65	990	N/A	−10
1980	Karl	28 Nov	45.0	−32.0	1	65	990	N/A	+
1981	Cindy	05 Aug	44.1	−50.4	1	40	1006	N/A	−4
1981	Dennis	22 Aug	37.8	−59.7	1	40	1003	N/A	−8
1981	Emily	11 Sep	42.7	−41.0	2	35	1005	+	+
1981	Harvey	19 Sep	38.3	−40.6	4	35	1005	+	+
1981	Irene	02 Oct	45.1	−25.0	4	50	999	N/A	0
1982	Debby	20 Sep	51.5	−19.0	1	50	996	N/A	+
1982	Ernesto	03 Oct	32.0	−58.0	1	45	1001	N/A	+
1982	Subtrop1	20 Jun	45.4	−56.0	1	60	984	N/A	+
1983	Alicia	20 Aug	36.5	−99.4	5	20	1010	0	0
1984	Cesar	02 Sep	46.2	−48.9	1	50	994	−5	−5
1984	Diana	16 Sep	46.0	−57.8	1	60	994	N/A	−12
1984	Josephine	18 Oct	44.0	−57.1	10	50	995	+	−2
1984	Klaus	13 Nov	42.0	−47.0	1	50	988	N/A	−10
1985	Ana	19 Jul	46.0	−57.6	2	60	996	N/A	−8
1985	Claudette	17 Aug	44.5	−22.5	1	40	1003	N/A	+
1985	Danny	19 Aug	36.7	−77.9	8	25	1012	0	−1
1985	Gloria	28 Sep	45.5	−70.0	17	75	964	−4	−23
1985	Juan	01 Nov	35.2	−86.6	2	35	986	N/A	+
1985	Kate	23 Nov	33.5	−70.5	1	35	1006	N/A	−1
1986	Charley	21 Aug	41.6	−56.6	22	40	1005	−25	−25
1986	Earl	19 Sep	43.5	−46.3	5	65	990	+	−5
1987	Arlene	24 Aug	50.0	−30.0	17	65	988	+	N/A
1987	Cindy	10 Sep	42.5	−28.0	1	35	1007	N/A	−13
1987	Dennis	20 Sep	32.8	−49.5	1	25	1012	N/A	−23
1987	Emily	26 Sep	49.0	−36.0	1	65	983	N/A	−33
1987	Floyd	13 Oct	28.1	−75.4	2	45	996	N/A	+
1988	Alberto	08 Aug	49.0	−60.0	2	35	1006	N/A	+
1988	Gilbert	19 Sep	40.2	−89.9	2	25	999	−4	+
1988	Helene	30 Sep	55.0	−30.0	1	65	990	N/A	N/A
1988	Keith	24 Nov	34.0	−66.0	9	60	990	−45	−52
1989	Allison	28 Jun	31.1	−94.2	15	30	1004	+	−2
1989	Felix	09 Sep	46.5	−35.5	5	37	1002	−7	−7
1989	Gabrielle	13 Sep	43.8	−51.5	1	30	1010	N/A	−15
1989	Hugo	23 Sep	42.2	−80.2	11	40	987	−13	−32
1990	Bertha	02 Aug	46.0	−60.0	2	70	973	N/A	−3
1990	Edouard	11 Aug	39.1	−22.0	9	30	1010	+	−3
1990	Gustav	03 Sep	48.5	−44.5	1	55	993	N/A	−7
1990	Isidore	17 Sep	50.0	−39.5	1	35	1005	N/A	+
1990	Lili	15 Oct	44.9	−61.0	3	45	995	N/A	−7
1990	Marco	12 Oct	32.0	−83.0	5	20	1004	+	+
1991	Bob	20 Aug	48.4	−61.9	44	45	998	−6	−6
1991	Claudette	12 Sep	34.3	−33.1	9	30	1012	+	+
1991	Erika	12 Sep	38.8	−23.3	2	30	1009	N/A	+
1991	Fabian	16 Oct	26.5	−78.5	2	40	1007	N/A	−5
1991	Grace	29 Oct	32.5	−59.0	1	85	982	N/A	+
1992	Bonnie	01 Oct	39.0	−22.8	8	40	1002	+	+
1992	Charley	27 Sep	40.4	−24.4	6	55	981	−1	−5
1992	Earl	03 Oct	28.4	−62.9	1	30	1008	N/A	−6
1992	Frances	27 Oct	47.6	−42.7	12	55	989	+	+
1993	Emily	06 Sep	39.8	−49.4	1	25	1013	N/A	+
1993	Floyd	10 Sep	47.3	−37.8	10	65	990	−24	−29
1993	Harvey	21 Sep	46.0	−42.0	1	50	997	N/A	+

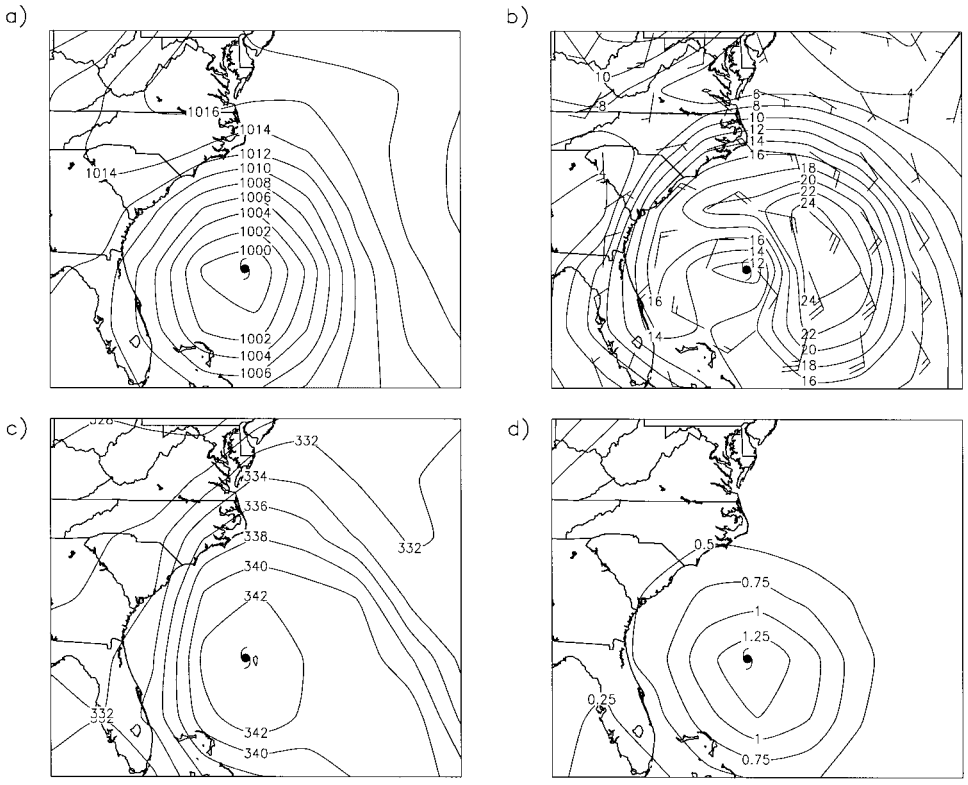

FIG. 1. Example of the representation of a tropical cyclone [Hurricane Gloria (1985)] within the ECMWF 2.5° Reanalyses fields. (a) Sea level pressure (hPa), (b) 925-hPa wind field (m s^{-1}), (c) 400-hPa equivalent potential temperature (K), and (d) 320-K potential vorticity (pvu).

seen in these fields (Fig. 1; see also Molinari and Vollaro 1989, 1990; Molinari et al. 1995). ECMWF analyses of Hurricane Gloria (1985) are shown in Fig. 1. While the core pressure of the storm clearly is underestimated (by 40 hPa here), despite being located offshore far from a rawinsonde site, the asymmetric wind field and warm core nature of the storm are satisfactorily captured by the 2.5° analyses.

Given the coarse resolution of the ECMWF dataset, it is clear that this dataset could not provide accurate absolute values of intensity during and after the transition phase. During such cases, the ECMWF reanalysis data are used to estimate intensity changes rather than absolute intensity values during the extratropical phase. The cyclone intensity as given by the ECMWF reanalyses is tracked with time prior to and following the NHC transition point. The ECMWF analyzed minimum sea level pressure after transition is then compared to the ECMWF analyzed pressure during the last report of the tropical phase. The difference between these two values represents the post-transition intensity change estimate. Statistics on all transitioning tropical cyclones during the 15-yr reanalysis period are summarized in Table 1. It is important to point out that the intensity-change estimates derived from the ECMWF reanalyses must be used with caution. While the analyses are able to estimate reasonably well the intensity of extratropical cyclones given their weaker pressure gradients and broad circulation, the same is not true for tropical cyclones. Given the strong pressure gradients and smaller scale associated with tropical cyclones, the 2.5° ECMWF reanalyses often greatly underestimate the intensity of the tropical cyclones. As a result, the intensity change estimates are likely to have an error associated with them that can be large for smaller transitioning tropical cyclones. Acknowledging this, for the majority of the text only the sign of the estimated post-transition intensity change is interpreted. The exception is in section 5 and Fig. 9, during which the actual intensity change magnitudes are used explicitly, keeping the caveats mentioned above in mind.

Daily rainfall records from the National Climate Data Center for 290 U.S. land-based stations (Fig. 3c) from 1945 to the present are used to calculate return periods of tropical cyclone–related rainfall. For the purposes of this study, any rainfall that fell at a station when a tropical cyclone was within 500 km of that station was deemed to be associated (even if only in part) with the tropical cyclone. This radius was chosen as it is sufficiently large to capture spiral rainbands well from the storm center, but not too large that rainfall from other systems beyond the tropical cyclone subsidence zone is included. This radius is comparable to the upper limit of the radius of gale force winds typically found in

cyclones that have completed extratropical transition (Elsberry 1995).

Finally, 1.0° × 1.0° Atlantic SST is examined using Reynolds weekly averaged SST fields (Reynolds and Smith 1995).

3. Impacts of tropical cyclones in the midlatitudes

The impact of tropical cyclones extends far beyond the tropical or subtropical latitudes. To elucidate the effects of tropical cyclones over the entire North Atlantic region, the return periods for passage of 1) a tropical cyclone and 2) a transitioning tropical cyclone within 111 km (60 nmi) of a given location are plotted in Fig. 2. Major midlatitude cities including Washington, D.C., New York, and Boston are all directly impacted by a tropical cyclone once or twice per decade, and by a tropical cyclone that has already transitioned every 1–2 decades. Statistics for western Europe are almost certainly higher than indicated in Fig. 2, since NHC typically discontinues tracking tropical cyclones well before they have reached Europe. Extrapolation of tracks for storms approaching Europe suggests that this region (as a whole) is impacted by a transitioning tropical cyclone every other year, on average. A careful reanalysis of historical data is needed to confirm this.

As numerous storms of the past century have shown us, the impact of a tropical cyclone extends well beyond a radius of 111 km. Damaging winds, flooding rains, and coastal erosion can extend several hundred kilometers beyond the center of a tropical cyclone. This is especially true when a tropical cyclone has completed extratropical transition (Elsberry 1995). Acknowledging this, the storm radius of influence is increased from 111 to 300 km and the resultant return periods for cyclone passage are plotted in Fig. 2c (tropical phase) and Fig. 2d (extratropical phase). All of the major cities mentioned earlier are threatened by a tropical cyclone (whether tropical or extratropical) every 2–4 yr.

While the statistics in Fig. 2 are useful for comparing relative threat for different regions of the basin, they do not give a practical measure of impact. The practical impact of tropical cyclones over the United States can be quantified by examining return periods for heavy rainfall events associated with tropical cyclones (Fig. 3). Heavy rainfall events are defined as either 1) 5 cm of rain from a storm or 2) 10 cm of rain from a storm. Only stations with at least 25 yr of daily precipitation data are used to derive these return periods (290 stations, shown in Fig. 3c). Most major cities in the northeast United States experience 5-cm rainfall from a tropical cyclone every 3–6 yr (Fig. 3a), and 10-cm rainfall from a tropical cyclone every 10–20 yr (Fig. 3b), typically falling within a 24–48-h period.

The impact of orography on these return periods is well illustrated in Fig. 3. The local minima of flood threat in eastern Tennessee and Kentucky and northwest Pennsylvania are the result of the terrain slope upwind of these regions. Since tropical cyclones most often pass to the east of these locations, the mountainous terrain effectively decreases the precipitation for leeward regions. In contrast, regions to the east of the Appalachians experience enhancement of precipitation when a tropical cyclone passes to the east. This is clearly evident in eastern Pennsylvania and central North Carolina (Figs. 3a,b). A documented example of the dramatic impact of orography on tropical cyclone structure and rainfall distribution is given by DiMego and Bosart (1982a,b).

Previous observational studies have shown that the radii of gale (17 m s^{-1}) and hurricane (34 m s^{-1}) force winds increase significantly during and following the transition process (Elsberry 1995). Thus, the areal coverage of strong or damaging winds associated with a transitioning or transitioned cyclone is often far greater (2–3 times) than a tropical cyclone of equal intensity. In addition, transitioning storms at higher latitudes move more quickly than those at lower latitudes. This increase in translational speed is added to the wind field, resulting in a highly asymmetric wind structure (Fig. 1). In this way, rapidly moving midlatitude transitioning storms with relatively high pressures (>980 hPa) may still produce exceptionally high wind speeds. The 1938 New England Hurricane (Pierce 1939), Hurricane Charley (1986), and Hurricane Luis (1995) are examples of such storms (Table 1). While transitioning storms at higher latitudes move more quickly than tropical cyclones at lower latitudes, the duration of gale or storm force winds at any one point can be larger since the wind radii often increase by a larger percentage than does the translational speed.

4. Spatial and temporal distribution of extratropical transition

a. Statistics and track analysis

Forty-two percent (355/841) of all Atlantic tropical cyclones occurring from 1899–1996 were classified by NHC as extratropically transitioning (Fig. 4a). This is slightly higher than the ratio found for the western North Pacific (36%; Klein 1997). For the period 1950–96 (a more uniformly reliable record; see Landsea 1993), 46% of all tropical storms (213/463) transitioned (Fig. 4b). Over the same 37-yr period 206 storms made landfall north of 25°N (United States, Canada, or Europe) of which 102 transitioned. Thus, 50% of landfalling storms ultimately underwent transition. The implications of these events are discussed in section 3 (see also Figs. 2 and 3). Clearly transition of tropical cyclones is significant across the wider Atlantic basin (including North America).

In this section, long-term average statistics for each month of the hurricane season are summarized. The seasonal distribution of the tracks of all extratropically transitioning cyclones since 1899 is plotted in Fig. 5. The

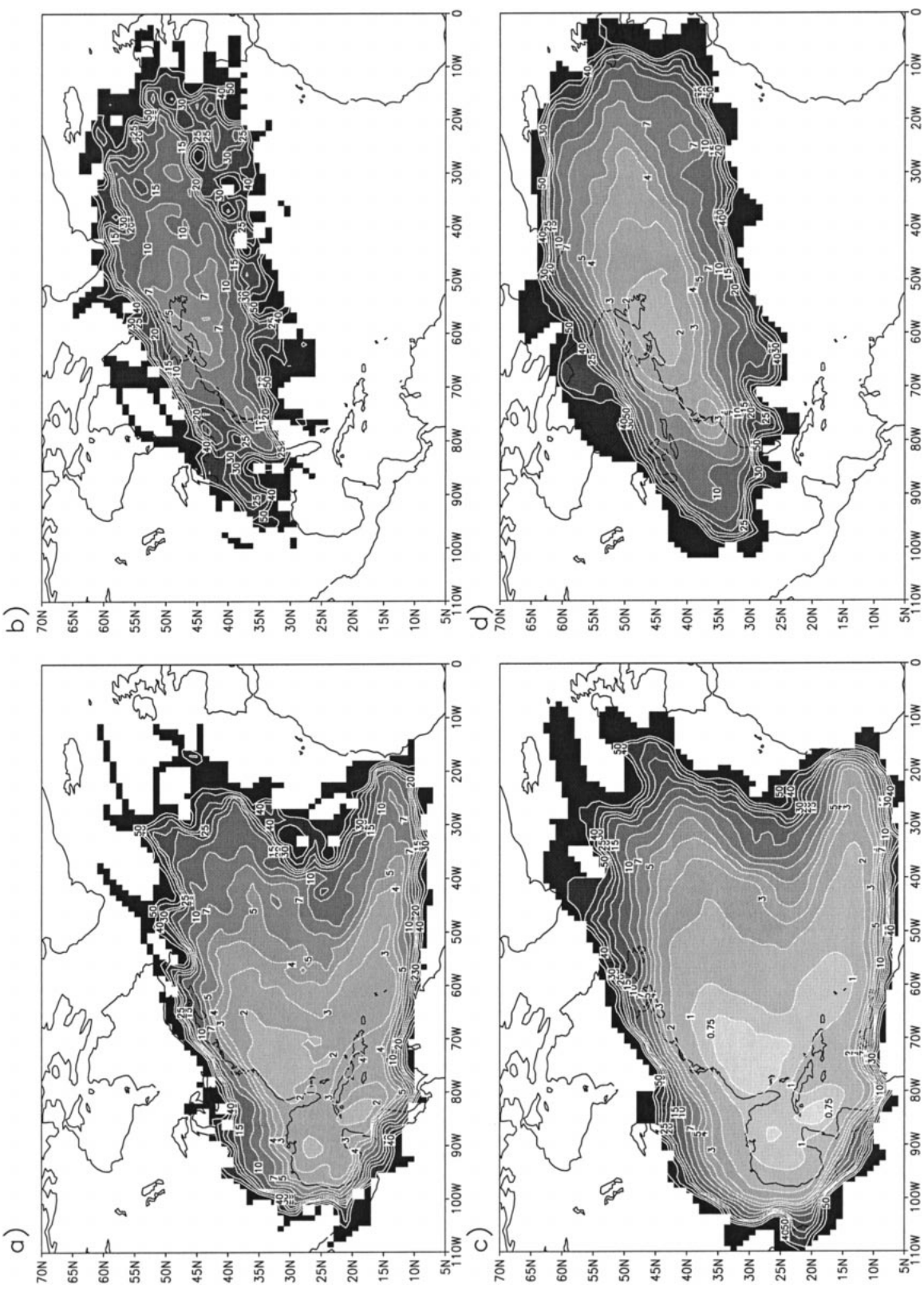

FIG. 2. A measure of the climatological impact of tropical cyclones on the midlatitudes. (a) The mean return period in years of a tropical cyclone passing within 111 km (60 nm) of a location. (b) Same as (a), except for extratropical phase. (c) Same as (a), except for passage within 300 km. (d) Same as (b), except for passage within 300 km. Both figures use NHC tropical cyclone tracks from 1899–1996.

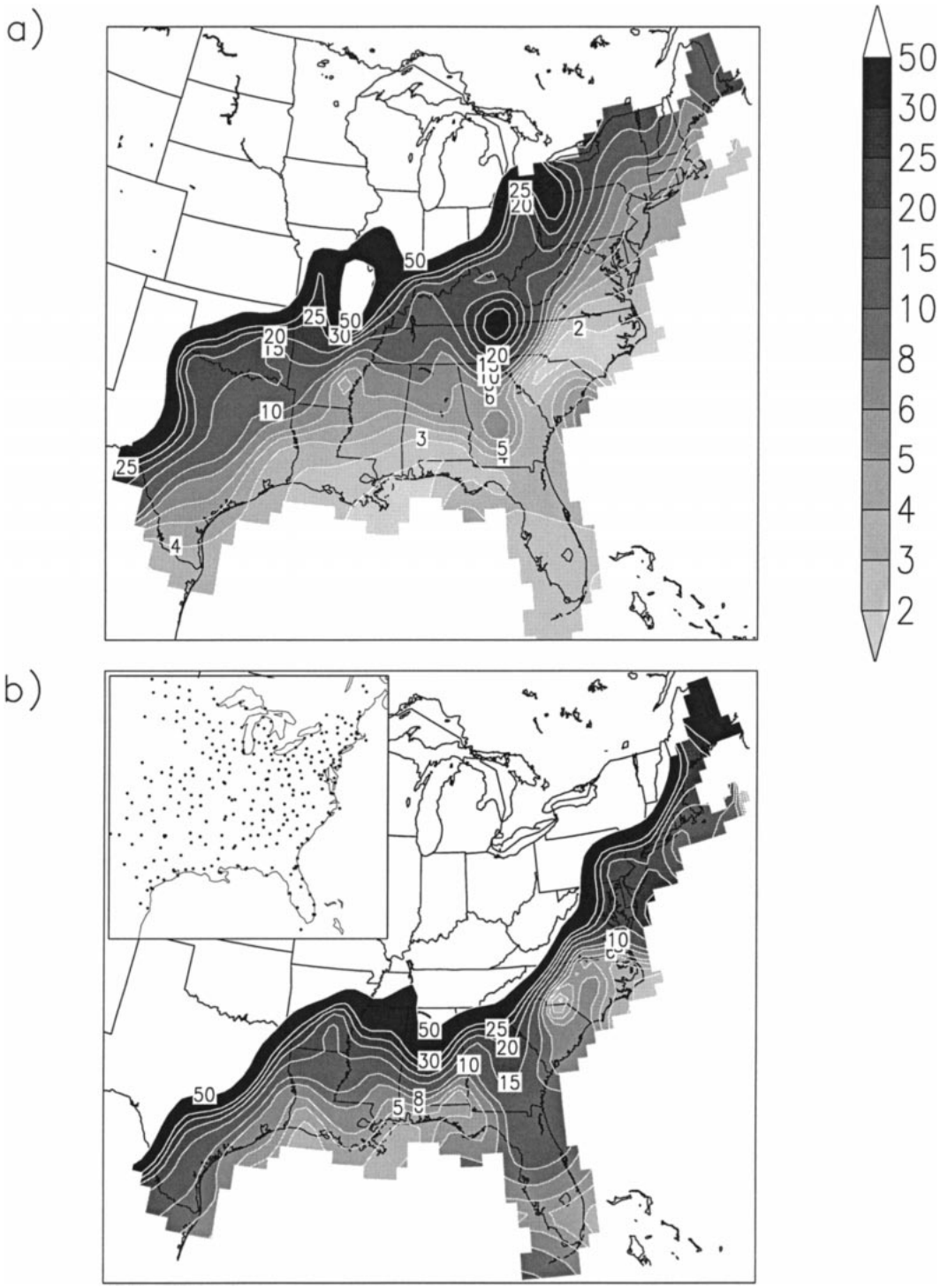

FIG. 3. A measure of the hydrologic impact of tropical cyclones in the United States. (a) The mean return period in years of a tropical cyclone producing 5 cm (2 in.) of rainfall, typically within 24–48 h. (b) Same as (a), except for 10 cm (4 in.). Both figures use tropical cyclone tracks and land-based precipitation data from 290 stations, shown in the smaller inset panel within (b), from 1930–96.

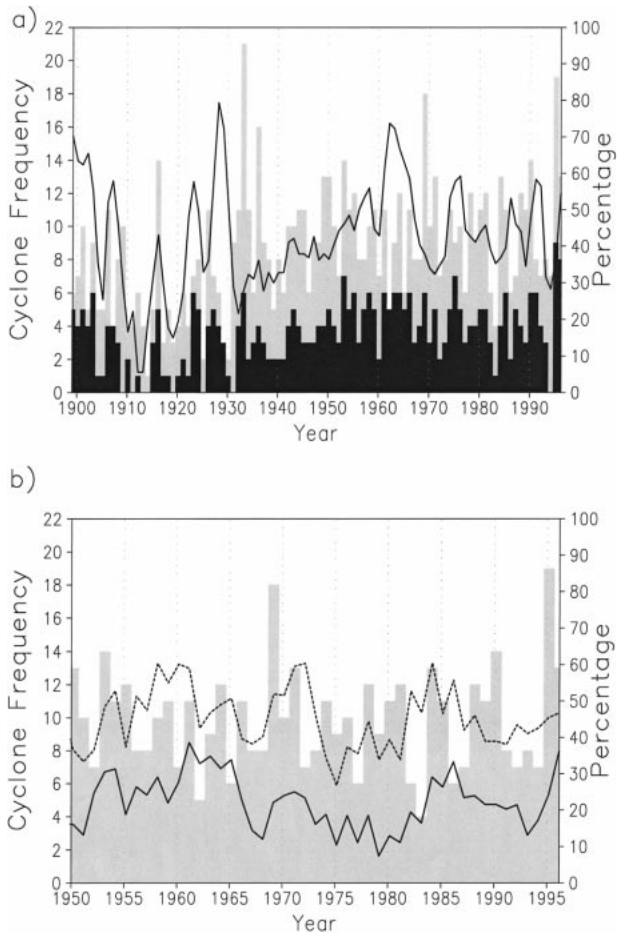

FIG. 4. (a) Annual frequency of Atlantic tropical cyclones (light shading) and transitioning tropical cyclones (dark) from 1899–1996. Solid line is a 3-yr running mean of percentage of tropical cyclones that transitioned. (b) Annual frequency of tropical cyclones is repeated (light shading) for the period 1950–96. Three-year running mean of the percentage of tropical cyclones that made landfall is given by the dashed line. The solid line is a 3-yr running mean of the percentage of all tropical cyclones that both made landfall north of 25°N and transitioned at some point in their life.

solid circles represent the point of transition as defined by NHC. Close examination of these tracks reveals a seasonal variation in the latitudinal band over which transition occurs. This seasonal fluctuation is summarized in the last panel in Fig. 5, which depicts the latitudinal mean, first and third quartiles, and extreme range of transition location by month.

During May and June, transition occurs at the lowest latitudes on average. By July, the mean latitude of transition shifts northward 5° latitude (a statistically significant shift of mean transition latitude to 99% confidence), well into the midlatitudes. Between July and September, transition occurs predominantly between 40° and 45°N, with no statistically shift in the mean transition band. Another dramatic shift in the mean transition location is observed from September to October (to 99% confidence), with a shift southward of 4° and a slight expansion north and south in range. During November, the area of transition contracts but the mean does not change significantly from October. These patterns suggest that the transition season can be broken into three periods: a low-latitude quiet early season, a high-latitude active midseason, and a midlatitude active late season. Features of the climate that contribute to this pattern are explored in section 4b.

Monthly frequency of transition (Fig. 6a, dark bars) correlates fairly well with the monthly number of tropical cyclones (Fig. 6a, light bars): a peak in August–October, with far less frequent occurrence prior to and following those months. The probability of transition (solid line in Fig. 6a) shows a gradually rising transition probability, peaking during the months of September and October when 50% of all Atlantic tropical cyclones transition (in the long-term mean). While transition becomes increasingly likely as the season progresses (Fig. 6a, solid line), this does not account for the fact that a significant number of storms that transition do not impact land. Figure 6b incorporates landfall into the transition statistics. The light shading in Fig. 6b is the frequency distribution of tropical cyclones repeated from Fig. 6a (light shading also). The medium shading in Fig. 6b tracks the monthly frequency of landfall in the United States, Canada, or Europe. The short-dashed line is the monthly percentage of tropical cyclones that made landfall (ratio of medium to lightest bars). Ignoring the month of May (which has only two transitioning cases over 97 yr), the percentage of landfalling storms decreases as the season progresses, consistent with the shift from the Gulf of Mexico and Caribbean developers early in the season to storms forming farther east in the open Atlantic late in the season (Fig. 5). The frequency of landfalling cyclones that transitioned is represented by the darkest shading in Fig. 6b. The long-dashed line is the percentage distribution of landfalling storms that transitioned (the ratio of the darkest bars to the medium bars in Fig. 6b). While landfalling probability rapidly decreases as the season progresses (short-dashed line), when a storm does make landfall, it is far more likely to ultimately undergo transition (long-dashed line). As will be shown in the next section, this can be attributed to increased frequency of troughs and higher baroclinicity over land later in the tropical season.

b. Cause of seasonal fluctuations in transition location

The signal illustrated in Fig. 5 is clear: transition occurs at higher latitudes during the peak of the season and lower latitudes during the early and later months. Figure 6a illustrates further seasonality: a steadily rising probability of transition that peaks in October. While we may not yet fully understand the processes governing transition from one event to another, we can explain this climatological shift in transition probability and occurrence.

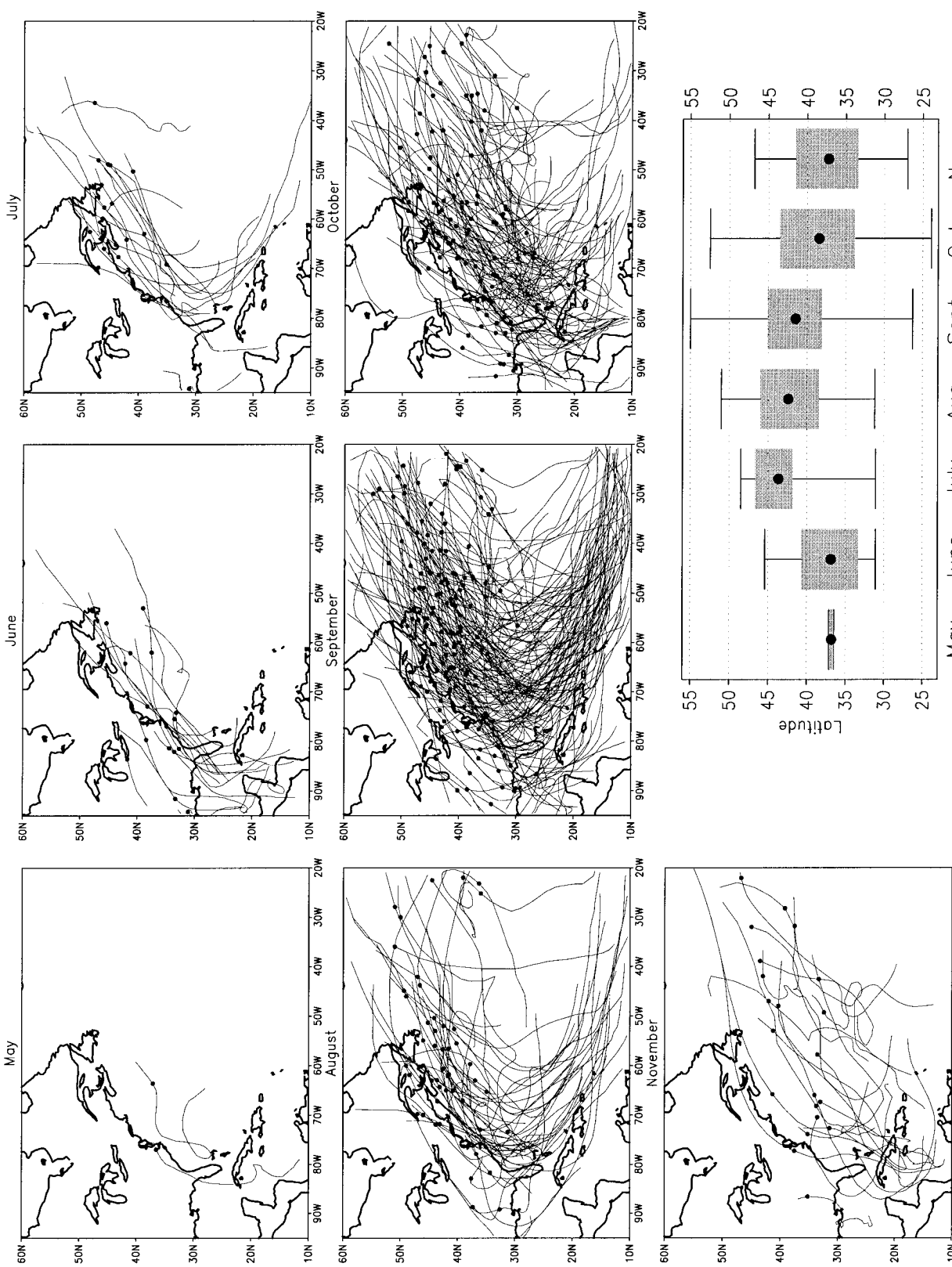

FIG. 5. Tracks of extratropically transitioning tropical cyclones by month. Dots represent the point of transition as defined by NHC. Bar chart represents a summary of the range of latitude over which transition occurs by month. The solid circles in the bar chart show the mean transition location for each month, while the lighter bars represent the latitudinal range of transition (first and third quartiles). The extreme latitudes of transition are represented by the horizontal bars beyond the first and third quartiles.

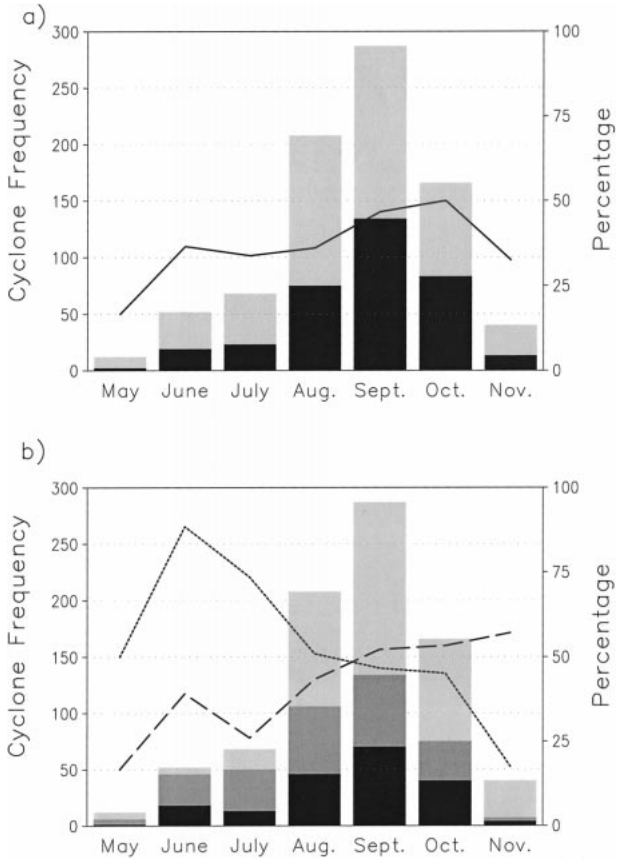

FIG. 6. (a) Annual cycle of the frequency of Atlantic tropical cyclones (light shading) and extratropical transition (dark shading) as a function of month. Solid line is the percentage of tropical cyclones that transitioned by month. (b) Annual cycle of tropical cyclone frequency is repeated (light shading). The medium shading shows the frequency of tropical cyclones that made landfall north of 25°N and the short-dashed line is the percentage of tropical cyclones that made landfall north of 25°N (medium/light). Darkest shading shows the frequency of landfalling tropical cyclones that also transitioned. Long-dashed line is the percentage of tropical cyclones that made landfall north of 25°N and transitioned.

Key diagnostics that summarize the monthly mean patterns found in Figs. 5 and 6 are plotted in Fig. 7. The fields shown are derived from the ECMWF reanalysis data for 1985. This year was chosen as the mean climate indices [Southern Oscillation index (SOI), North Atlantic oscillation (NAO), and Pacific–North American index (PNA)] were all nearly neutral during the hurricane season. The thick dotted contour is the 960-hPa monthly mean theoretical maximum potential intensity (MPI) for a tropical cyclone. The MPI is calculated using a Carnot-engine thermodynamic assumption for a tropical cyclone (Emanuel 1988; Bister and Emanuel 1998), assuming ideal efficiency (shear and asymmetries are ignored). This boundary is a first-order measure of the northern climatological boundary at which purely tropical intensification is no longer possible (according to current interpretation of tropical storm processes). Thus, this contour is approximately the boundary north of which tropical cyclones typically will either decay rapidly and/or transition. This boundary changes with time as both the ocean and upper-atmosphere temperatures change with time, and thus changes in the convective available potential energy. This latitudinal shift of this boundary from month to month (Fig. 7) provides one regulator (the tropical regulator) of the seasonal cycle found in Fig. 5. A second regulator of the seasonal cycle in Fig. 5 is the extratropical regulator. This can be described by the 700-hPa climatological growth rate (σ) for baroclinic instability from the Eady model of instability (shaded field in Fig. 7),

$$\sigma = 0.31 f U_z N^{-1}. \quad (1)$$

Here, f is the Coriolis parameter, U_z is the vertical shear of the horizontal wind, and N is the Brunt–Väisälä frequency. The light and dark shaded regions correspond to 0.25 and 0.5 day^{-1}, respectively. This parameter was used by Hoskins and Valdes (1990) to interpret the climatology of baroclinic wave growth in midlatitude storm tracks and the values contoured here are representative of the most baroclinically active regions of the world (Hoskins and Valdes 1990). Baroclinic growth rate is used here to illustrate the month-to-month movement of the most climatologically favored regions for baroclinic development as it pertains to extratropical transition, hence the term extratropical regulator. As one would expect, early in the season baroclinic instability is weak and confined north of 40°N. By August, this region begins moving southward, intensifies rapidly in September and dominates the midlatitude climate by November.

Thus, we are presented with two fields that compete: the MPI (dotted) acts to extend the tropical cyclone life cycle farther north into the Atlantic, while the baroclinically active region (shaded) acts to suppress it farther south. The synthesis of these two fields regulates extratropical transition, resulting to first order in the patterns of transition shown in Figs. 5 and 6. The region of cyclone decay (whether tropical or extratropical) can be denoted by the region between the 960-hPa MPI contour and the 0.25 day^{-1} σ contour. The larger the areas indicative of tropical decay (i.e., low σ and small MPI), the less likely extratropical transition is. This explains well the decreased transition probability found in June and July, where over 5° latitude separates these two boundaries (960-hPa MPI and 0.25 day^{-1} σ). Put simply, in the mean, tropical cyclones are not able to reach a baroclincally favorable region for development before weakening too greatly to survive transition. This will be examined in more detail in section 5. By August, however, the 960-hPa MPI and baroclinic development regions coincide along the Gulf Stream near 65°–75°W (in the long-term mean). Superposition of these regions continues to expand eastward through September and October, illustrating the increased probability of transition. The long-lived superposition of these boundaries

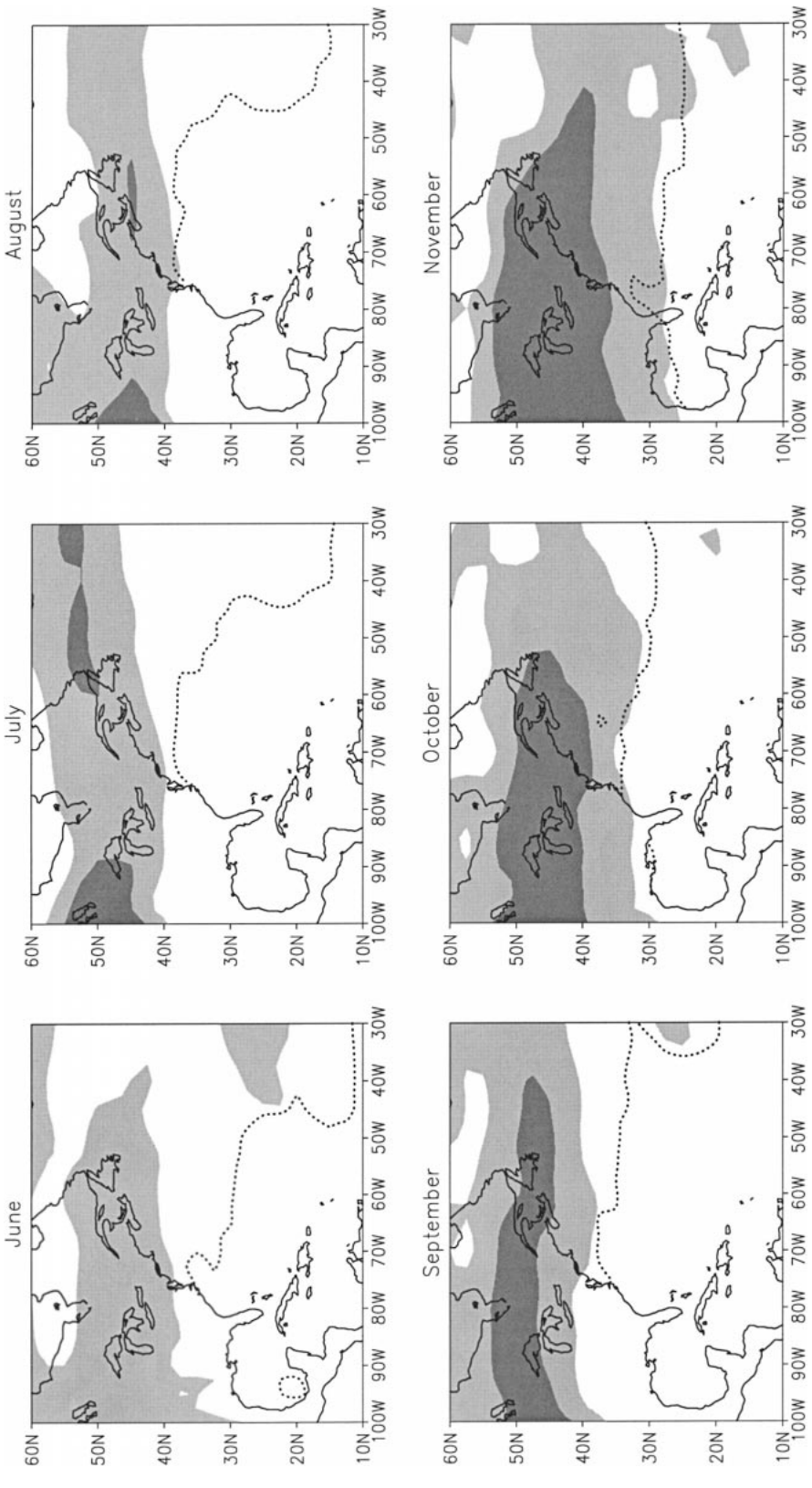

FIG. 7. Explaining the seasonal cycle in transition frequency and location. Dotted line denotes climatological regions of support for tropical intensification (minimum pressure of 960 hPa from MPI theory). Shading is the Eady baroclinic growth rate parameter (σ) from 1985 monthly mean 700-hPa ECMWF 2.5° reanalyses (light and dark shaded at 0.25 and 0.5 day^{-1}, respectively). Here $\sigma = 0.31 f U_z N^{-1}$, f = Coriolis parameter, U_z = vertical derivative of the horizontal wind, N = Brunt–Väisälä frequency.

(960-hPa MPI and 0.25 day^{-1} σ) along the western Atlantic also illustrates the threat of transitioning storms to New England and the Canadian Maritimes. In these cases, transition rapidly follows the tropical intensification phase with only a short period (if any) of tropical decay. The patterns in Fig. 7 also suggest an explanation for the observed intensity changes associated with the life cycle of transitioning storms (discussed in detail in section 5).

It should be noted that whether a specific tropical cyclone transitions (and if so, whether it intensifies after transition) depends largely upon the structure of the local MPI and baroclinic growth rate fields for that specific period. Although September and October are climatologically most favored for transition, there are certainly many cases where the transient atmospheric and oceanic structures do not support transition during a specific storm.

5. Intensity changes during and after extratropical transition

Positive feedback processes [e.g., the Wind-Induced Surface Heat Exchange mechanism, (Emanuel 1986)] can produce tropical cyclones of extreme intensity (e.g., SLP $<$ 960 hPa). Such extreme intensities can result (if a storm continues to move over warm water and avoids upwelling and shear) since the primary factor limiting intensity is frictional dissipation, which is a relative minimum over the ocean. Bister and Emanuel (1998) have shown that the frictional heat source can lead to significant intensification of tropical cyclones (maximum wind speed increased by 20%). However, since frictional heating is proportional to $v^{1.5}$, and frictional dissipation is proportional to v^3, frictional drag ultimately bounds the tropical cyclone intensity. In contrast, extratropical cyclones are, by definition, removing the instability that created them. Thus, while a far greater amount of potential energy may be available to extratropical cyclones, they cannot achieve the extreme intensities found by tropical cyclones. This contrast in energetics ensures that the minimum pressure attained by tropical cyclones is typically much lower than minimal pressures attained by extratropical cyclones. Therefore, when a tropical cyclone does transition, the pressure attained by the transitioned storm rarely reach the minimum pressures found during the tropical phase.

a. Distribution of post-transition intensity change

A scatterplot of the minimum tropical cyclone pressure during the tropical phase compared to the minimal pressure attained during the extratropical phase (Fig. 8a) illustrates this effect. With the exception of 14 storms (those in the shaded half of Fig. 8a), the vast majority of transitioning storms in this 97-yr period never regain the minimum pressures observed during their tropical phase. These 14 storms (13% of transitioners during the

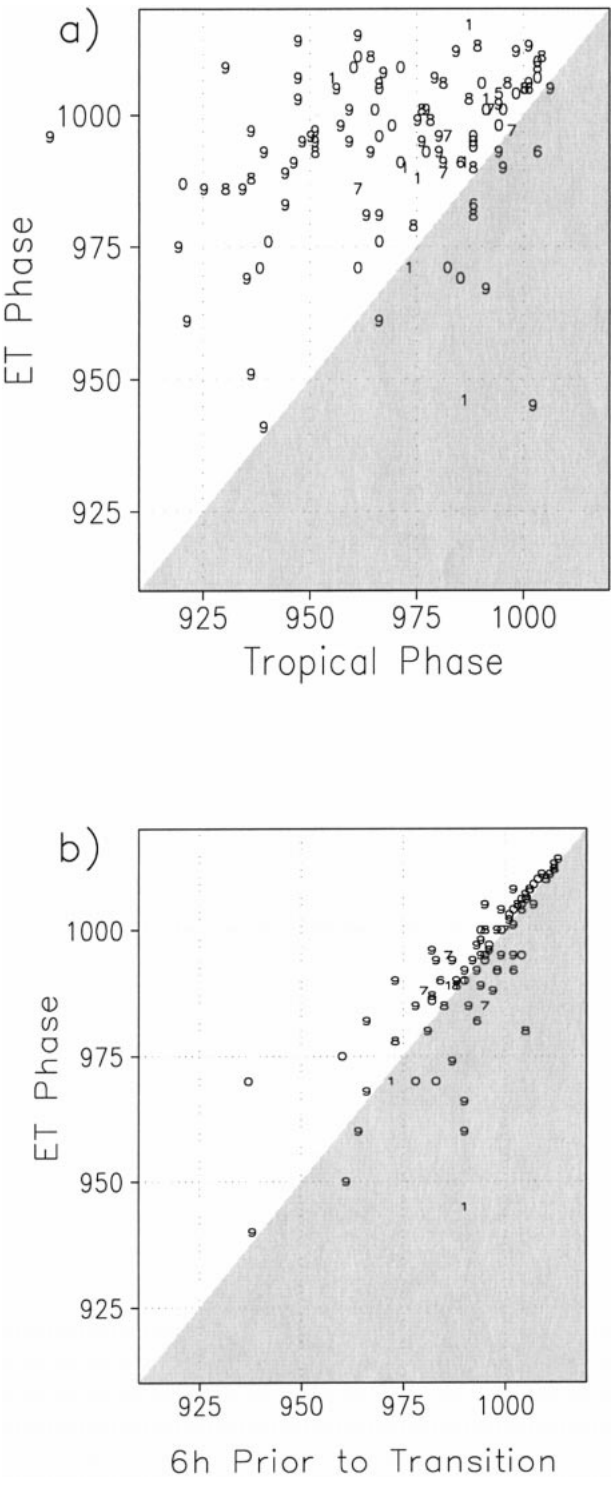

FIG. 8. (a) Scatteplot of the distribution of peak cyclone intensities during the tropical and extratropical phases. The minimum pressure attained during the tropical phase is plotted against that attained during the extratropical phase. (b) Scatterplot of tropical cyclone intensity change after transition. The intensity 6 h prior to transition is plotted against the peak intensity attained after transition. Both figures use NHC best-track data from 1899 to 1996. In both figures, the number plotted represents the month of the year the storm transitioned (e.g., 6 = Jun, 9 = Sep, 1 = Nov).

97-yr period), represent the anomalies and are worthy themselves of examination, in terms of the environments (both synoptic and mesoscale) that allowed them to intensify beyond their maximum tropical state.

In the 6 h preceding transition, 45% of tropical cyclones are of hurricane intensity, 45% are tropical storms, and 10% have weakened to depression stage. During and after extratropical transition, a cyclone usually weakens first, but may subsequently intensify rapidly. The radius of gale force winds is frequently observed to expand markedly (Elsberry 1995). Hence, a transitioning tropical cyclone has, associated with its developing extratropical kinetic energy field, the potential to produce structural damage upon land areas and significant coastal erosion and storm surge upon coastal areas.

Following transition, most tropical cyclones undergo substantial intensity changes (evident as a spread away from diagonal axis in Fig. 8b). Despite the rapidly cooling water, 51% of tropical cyclones deepen compared to their pretransition intensity (shaded half in Fig. 8b). Of the remaining 49%, 42% of storms weaken after transition and 7% remain stable (± 2 hPa). Thus, the dominant mode of intensity change after transition is intensification. This may support the result of Palmén (1958) that the available potential energy (APE) of the atmosphere increases during the transition process, making the atmosphere more conducive to growth of baroclinic instability. The strong circulation of these storms (including the warm core itself) warms the air ahead of troughs and lowers the effective static stability [N in Eq. (1)], enhancing existing temperature gradients (and so APE).

b. Describing post-transition intensity change

The database of intensity change statistics for each month is small, making it difficult to identify any seasonal cycle of intensity changes undergone by a transitioning tropical cyclone. Therefore, defining strong relationships between post-transition intensity change and Fig. 7 are not possible. For the dataset used here, slightly higher probabilities of post-transition intensification were observed during August–October than during May–June. Examination of the spatially varying MPI and baroclinic growth rate fields on a case-by-case basis shows promise in explaining the variability in post-transition intensity change. The results of this analysis are shown next.

In section 4b it was argued that the probability of transition is related to the displacement between the region supporting tropical development (960-hPa MPI) and the region supporting extratropical development ($\sigma > 0.25$ day^{-1}). We can extend this argument such that intensity changes late in the tropical cyclone life cycle (post transition) can be compared to the measure of the displacement between these boundaries. Figure 9a shows the relationship between the transit time a tropical cyclone required to travel the distance between the two aforementioned boundaries, and the post-transition intensity change. Negative intensity change indicates intensification (in hPa), and negative transit times indicate the anomalous case where the tropical cyclone crossed the $\sigma = 0.25$ day^{-1} boundary before crossing the MPI $= 960$ hPa boundary. These negative transit time cases could be qualitatively described as cyclones within a hybrid environment—where both tropical and extratropical forcing support intensification. From Fig. 9a, we can conclude that, on average, the less time the cyclone takes to cross the nonsupportive region, the greater the post-transition intensification. This relationship holds true for both straightforward (positive transit time) and hybrid (negative transit time) transition cases. Exponential regression analysis on the *subset of post-transition intensifying storms* within Fig. 9a reveals a correlation of -0.71, suggesting a strong exponential relationship. This corresponding relationship between intensity change (ΔP, in hPa) and transit time (T, in hours) is $\Delta P = -a^{*}b^{T}$, where $a = 16.36$ and $b = 0.976$.

Further examination of Fig. 9a reveals clustering of the pairs into three groups: 1) transit time above about 70 h (little, if any, reintensification); 2) transit time of less than 55 h with low–moderate reintensification ($|\Delta P| < 20$ hPa); and 3) short transit times (<24 h) with strong intensification. Comparison of the storms found in Fig. 9a with their peak tropical intensity (Table 1, also plotted in Fig. 9b) shows that both tropical storms and intense hurricanes can intensity after transition. For example, Keith (1988) had a maximum tropical intensity of 990 hPa and yet intensified 52 hPa after transition; and Hugo (1989) had a peak tropical intensity of 918 hPa and intensified 32 hPa after transition (Fig. 9b). However, there are notable characteristic differences in transit time required. With the exception of two storms [Bob (1991) and Emily (1987)], all tropical cyclones having a tropical-phase minimum pressure greater than 970 hPa required less than 20 h of transit time to enter a baroclinically favorable region and intensify thereafter (Fig. 9b). In contrast, nearly two-thirds of post-transition intensifying storms having a tropical-phase minimum pressure less than 970 hPa endured more than 20 h of transit time. Further, only 2 of the 14 post-transition intensifying storms with a tropical-phase minimum pressure of 990 hPa or greater had a transit time greater than 20 h. This suggests that tropical systems that are more intense in the tropical phase are able to survive for a greater period of time in the nonsupportive region (between 960-hPa MPI and $\sigma = 0.25$). Weaker tropical systems are able to intensify after transition, if they can quickly enter a supportive baroclinic environment after leaving the unsupportive tropical environment.

Despite the strong relationship found in Fig. 9, the results must be used with caution. The magnitudes of post-transition intensity change can depart significantly from actual values due to the resolution of the ECMWF reanalyses. Depending on ability of the analyses to re-

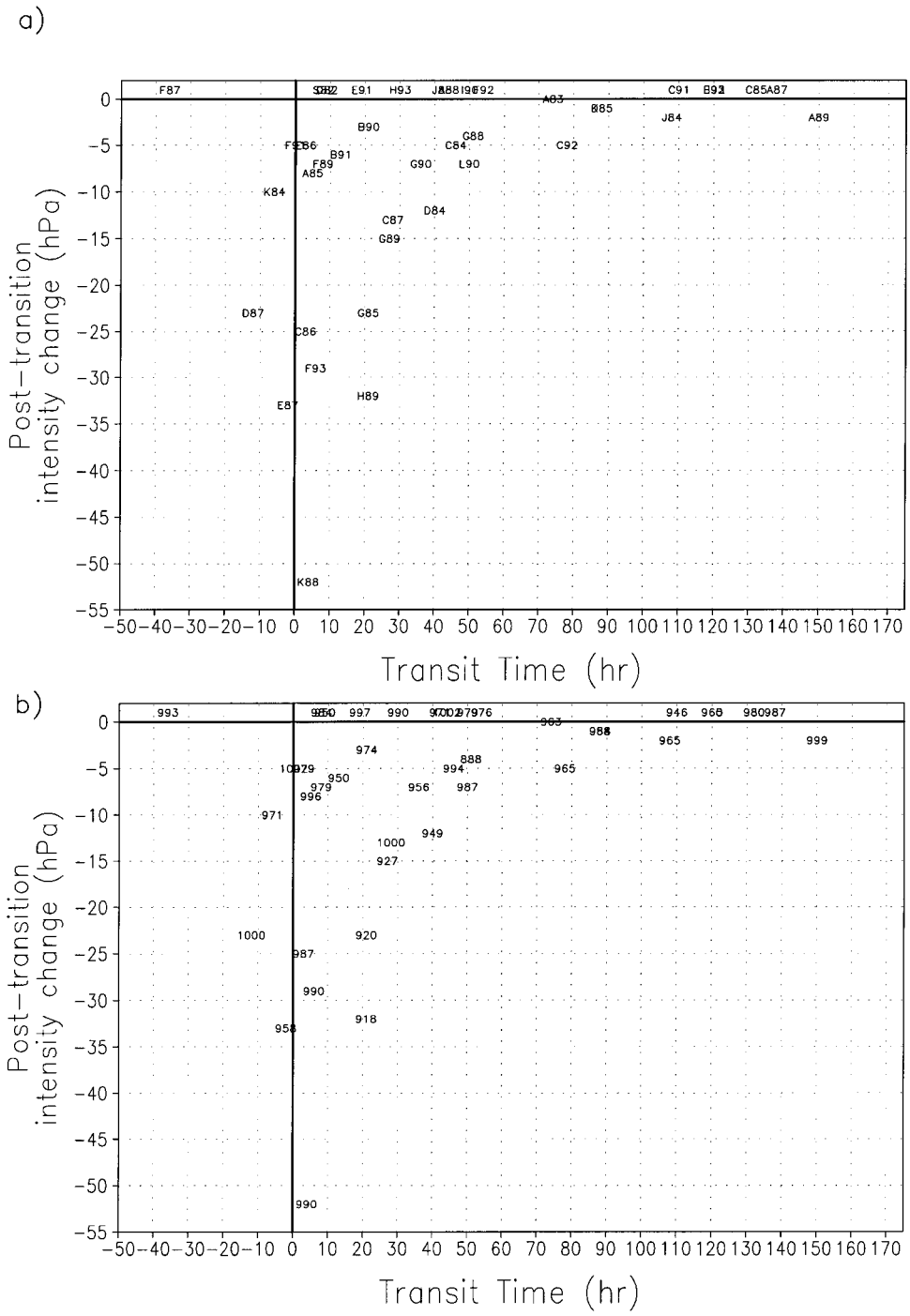

FIG. 9. (a) Scatterplot of post-transition intensity change as a function of transit time to cross the area between the tropically supportive boundary (960-hPa MPI) and the extratropically supportive region ($\sigma >$ 0.25 day^{-1}). The letter of the month and year of the storm are used as identifiers (e.g., K88 = Keith from 1988). Negative values of transit time indicate that the two regions overlap, and the tropical cyclone entered the extratropically supportive region *before* exiting the tropically supportive region. Post-transition intensity change was calculated using ECMWF 2.5° reanalysis data, where the maximum intensity after transition was compared to the intensity during the last 6 h of the tropical phase. Storms that weakened continuously after transition (14) were all given an intensity change value of +1 for qualitative purposes only. (b) Same as (a), except that the minimum pressure (hPa) attained by each cyclone during the tropical phase is plotted (corresponding to column 6 in Table 1).

solve either the tropical cyclone or extratropical cyclone, the actual post-transition intensity change can be underestimated or overestimated [Table 1, e.g., Frederic (1979), Gloria (1985), Hugo (1989)]. This likely accounts, in part, for the scatter found in Fig. 9 and the unexplained variance in the regression analysis performed previously.

6. Relationship between intensity change and transition, and formation locations

Figure 5 illustrated the seasonal cycle of extratropical transition for all transitioning cyclones. However, the storms in that analysis represented a wide spectrum of damage potential, threat, and forecast difficulty. The more difficult forecasting cases are often those where minimal tropical storms or hurricanes intensify after transition, becoming more dangerous than they were late in the tropical phase. Consequently, a useful factor for determining relative threat from a transitioning storm would be the post-transition intensity change used in section 5. We can gain insight into the spatial characteristics of this subset (and provide a basic understanding of where the most threatening transitioning cyclones originate) by examining their formation and transition locations (Fig. 10).

The subset of 1979–93 storms plotted in Fig. 10a are those where the transitioning cyclone intensified by more than 2 hPa below the pressure 6 h prior to transition (see also Table 1). Since the tropical cyclone is moving over cool or cold water at this point, any amount of intensification is deemed significant.[1] For this subset of storms, the point at which tropical storm status was reached is denoted by a cyclone symbol and the point of transition is denoted by ''L.''

Most post-transition intensifiers formed as tropical storms deep in the Tropics or in the warmest part of the Gulf Stream north of the West Indies (Fig. 10a). This might suggest that storms that have the most purely tropical origins and are the strongest (climatologically) are the most likely to undergo post-transition intensification. This supports the results found in section 5b, where intense tropical cyclones are more likely to survive the unsupportive region between the warm tropical waters and the baroclinic midlatitudes. Similarly, it could also suggest that when storms form in the deep Tropics, the large-scale pattern (several days to a week later, when transition occurs) favors post-transition intensification.

During the 15-yr period (1979–93), 45 tropical cyclones entered or formed within the Gulf of Mexico. Of these, 14 (31%) underwent extratropical transition at some point in their life cycle. None of these 14 transitioning storms underwent post-transition intensification; however, a few recent landfalling storms [e.g., Danny (1997)] have made transition. Landfall of a Gulf of Mexico tropical cyclone (and, effectively, an artificial 960-hPa MPI boundary in Fig. 7) occurs at low latitudes, such that extreme weakening of the cyclone usually occurs well before interaction with a baroclinic zone farther north can lead to post-transition intensification. Further, high pressure aloft and weak shear are required for the Gulf of Mexico tropical cyclone formation, both of which preclude the presence of strong baroclinicity soon after landfall. Hurricane Danny (1997) was able to survive intact after making landfall from the Gulf of Mexico. Danny (1997) moved offshore of Virginia, interacting with a developing trough and associated baroclinic zone to undergo transition east of New England.

It might have been expected that storms that have baroclinic characteristics at the time of genesis would be more likely to intensify baroclinically during and after transition. Superficially, we could speculate that such storms have a head start on the transition process. However, these results suggest the opposite. It would appear that the ''purely'' tropical systems having lower central pressures and taller cores represent more conducive potential vorticity anomalies for baroclinic development (Fig. 7) when moving into the midlatitudes. These anomalies (which are typically large departures from the midlatitude climatological mean for the time of year) advect unusually warm, moist air into high latitudes. This combination leads to a dramatic decrease in static stability, and a rise in the baroclinic growth rate [Eq. (1)]. Partial baroclinic characteristics initially may accelerate the transition process (e.g., Bosart and Bartlo 1991) since these storms form closer to the transition zone (e.g., light shading in Fig. 7). However, it appears that those characteristics inhibit the likelihood of post-transition intensification since these systems are less likely to have developed into a deep tropical cyclone prior to encountering a strong baroclinic zone. In these cases, the potential vorticity anomaly produced is only of moderate intensity and is far less likely to support accelerated development when interacting with a baroclinic trough in the midlatitudes. However, there are notable exceptions to this, including David [(1979); Bosart and Lackmann 1995].

The pattern of the transition locations (L) in Fig. 10a is consistent with the discussion from previous sections. For post-transition intensifiers, the dominant transition locations are within a narrow band between 37° and 47°N, with two extensions southward at 65° and 50°W, and a northward extension at 30°W. As mentioned earlier, the location of the maximum atmospheric baroclinic instability (and associated climatological long-wave trough axis and associated subtropical/polar jetstream) during the fall season may explain the pattern shown to some degree.

To complete the analysis, Fig. 10b presents the same dataset as Fig. 10a, except for the subset of tropical

[1] A threshold of 2 hPa was used to eliminate cases where the actual intensity was uncertain, and persistence may have been used to subjectively determine cyclone pressure.

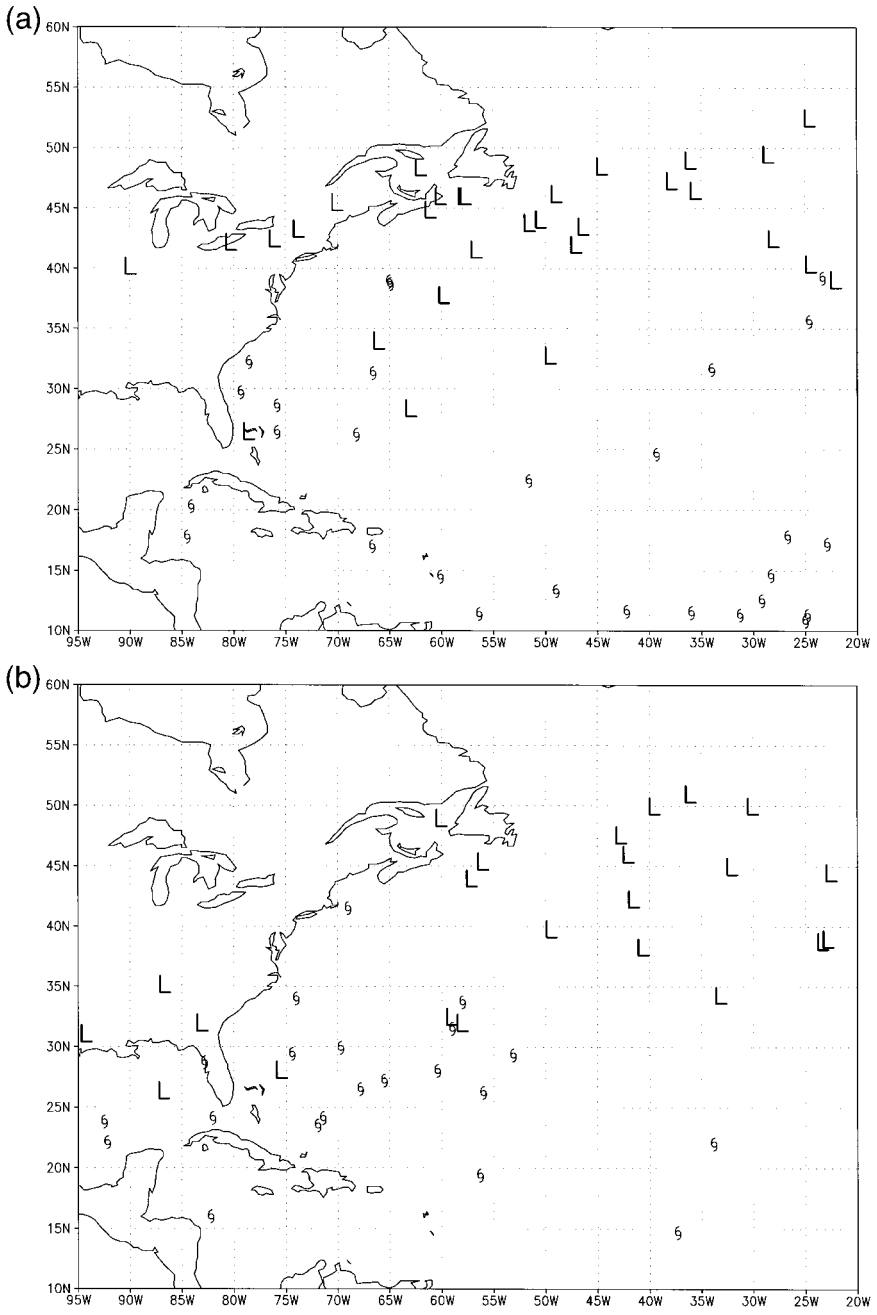

FIG. 10. Formation locations (§) and transition locations (L) of transitioning tropical cyclones. ECMWF 2.5° reanalyses data supplemented NHC best-track dataset for the period 1979–93. Data are for (a) storms intensifying after transition and (b) storm decaying post-transition.

cyclones that weakened after transition (and never recovered to pretransition intensity). These are the transitioning cyclones that typically pose a serious threat immediately after transition, with the threat decreasing with time. The tropical cyclone formation region for the post-transition weakeners is significantly different from the post-transition intensifiers. All post-transition weakeners during this period formed at or north of 15°N, (only one storm within the Cape Verde region) and 90% (22/25) formed north of 20°N. A large fraction of the weakeners formed in the western or central Atlantic. The transition region over eastern North America and the western Atlantic (Fig. 10b), is far less populated than in Fig. 10a. The dominant transition region for weakeners is the north-central Atlantic Ocean, with another transition region (albeit very sparsely populated) in the southeastern region of the United States.

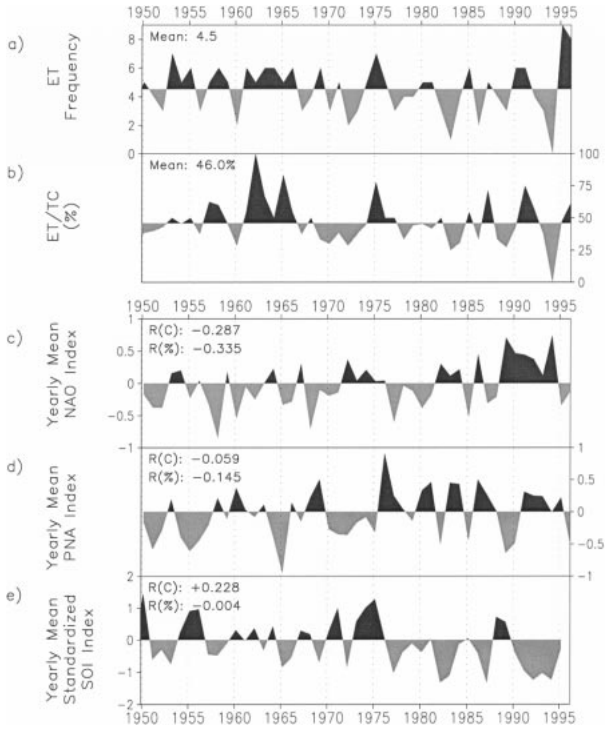

FIG. 11. Time series of (a) annual frequency and (b) percentage of all extratropically transitioning Atlantic tropical cyclones and three climatological indices: (c) yearly mean NAO index; (c) yearly mean PNA index; and (e) yearly mean standardized SOI. Here $R(C)$, linear correlation between the climate index and the yearly transition frequency (a) and $R(\%)$, linear correlation between climate index and the yearly transition percentage (b), are indicated in (c)–(e).

7. Extratropical transition frequency relationship with climatological indices

The frequency distributions of transition and transition percentage during this period are plotted in Fig. 11. Mean values are used as the baseline for determining above- or below-normal occurrence. These means are 4.5 transitions per year, representing 46.0% of the mean tropical cyclone yearly total. Peaks of transition occurrence and percentage were seen in the 1950s, early 1960s, the late 1970s, and sporadically during the 1980s and late 1990s. Since reliable tropical cyclone and transition frequencies and climate indices are not all available for years prior to 1950, the climate index correlation analysis here is limited to the period 1950–96.

Locations of the long-wave trough pattern (baroclinic instability; Fig. 7) and oceanic temperatures in the midlatitudes seem to play a significant role in determining where storms transition, the probability for intensification after transition, and speed of storm motion after transition (sections 4–6). Further, recent studies have shown a significant correlation between ENSO warm (cold) events and the decrease (increase) in Atlantic tropical cyclone frequency (Goldenberg and Shapiro 1996). These observations suggest that transition variability may be partly governed by changes in the basin-scale structure on interannual timescales. To examine this, frequency of extratropical transition is compared with relevant climatological indices. The three indices used as measures of the variability of the large-scale flow affecting North America and the Atlantic Ocean are 1) the NAO index (van Loon and Rogers 1978), 2) the PNA index, and 3) the standardized SOI (Troup 1965). Time series of the yearly mean of these three indices are plotted in Figs. 11c,d,e, respectively. In each case, zero is used to represent the neutral condition. Correlations between each of the NAO, PNA, and SOI indices and transition frequency time series in Figs. 11a,b are summarized by the $R(C)$ and $R(\%)$ values: $R(C)$ is the correlation between the transition frequency (Fig. 11a) and the plotted climate index; $R(\%)$ is the correlation between the transition percentage (Fig. 11b) and the plotted climate index. Interannual variability of extratropical transition frequency is partially described by the NAO index (Fig. 11c) and the SOI (Fig. 11e). When the NAO is in the positive phase, transition frequency is decreased. When the SOI is in the warm (ENSO) phase (SOI < 0), transition frequency is also decreased. The PNA index has insignificant correlation with transition frequency in the Atlantic Ocean; since the transition region is on the extreme eastern edge of the known range of influence of the PNA teleconnection pattern, this result is not surprising.

The relationship between the NAO and SOI with transition frequency may be attributable more to the relationship with the number of tropical cyclones than directly associated with the transition process itself. To minimize this effect, linear correlations of the transition percentage (Fig. 11b) with each of the climatological indicators are calculated, as they may be less dominated by the seasonal tropical cyclone frequency. The NAO has a stronger relationship with the transition percentage variability, suggesting it does play a moderating role in determining the probability of a tropical cyclone transitioning. The PNA and SOI have only slight negative relationships, as expected. None of these correlations is significant at the 95% level. These results suggest that several conventional measures of climatological variability (PNA, NAO, SOI) individually describe no more than about 10% of the observed year-to-year variability.

8. Summary

The findings of this research on the extratropical transition of Atlantic tropical cyclones can be summarized as follows.

- Extratropical transition in the North Atlantic basin occurs for 46% of all tropical cyclones. This is a higher percentage than that found for the northwestern Pacific basin (36%; Klein 1997).
- While landfall of a cyclone is most likely early in the season, transition of a cyclone is most likely late in the season (October is the month in which the per-

centage of tropical cyclones undergoing transition is at maximum).

- The coastline of the Atlantic basin is regularly impacted by transitioning cyclones. The major midlatitude cities of Atlantic coastal North America experience the effects of a tropical cyclone (whether tropical or transitioned) every 2–4 yr. These effects include 5–10 cm of 24–48-h rainfall several times a decade, gale to storm force winds, and significant beach erosion.
- Transition most often takes place at lower latitudes (30°–35°N) early and late in the season and at high latitudes (40°–50°N) during the peak of the hurricane season. This monthly cycle of transition location is the result of competing factors. The delayed warming of the oceans tends to force the location of transition northward, since the critical threshold for tropical development is pushed northward. Conversely, however, the climatologically favored region for baroclinic development and growth expands southward after August, encroaching on the oceanic area over which tropical development can occur, and pushing the region of most favored transition (suitable baroclinic growth rate) southward.
- Once tropical cyclones transition, they can undergo rapid intensity changes of either sign. Most of the post-transition intensifiers (51% of transitioning storms) form in the deep Tropics, especially within the Cape Verde region. Intensifiers also transition in a relatively confined latitudinal range of the Atlantic basin, focused around climatological long-wave and short-wave trough patterns and the polar jet axis. Storms undergoing post-transition decay (42%) most often form outside the deep Tropics (90% north of 20°N) and transition farther northeast than the intensifiers, or over land in the southeast United States. Consequently, it appears that having a strong baroclinic component early in the tropical development stage is detrimental to ultimately becoming an intense transitioned tropical cyclone.
- Around 50% (R of 0.71) of the post-transition intensity change variability can be described by the transit time a tropical cyclone requires to enter the region where extratropical development is supported ($\sigma > 0.25$ day^{-1}) after leaving the tropically supportive region (960-hPa MPI). Both weak and strong tropical cyclones can intensify after transition. However, weak tropical cyclones (MSLP $>$ 990 hPa) must enter a baroclinically supportive region soon ($<$20 h) after leaving a tropically supportive region if post-transition intensification is going to occur.
- Several conventional measures of climatological variability (PNA, NAO, SOI) describe no more than 10% of the observed year-to-year variability in the frequency of transition frequency and transition percentage.

9. Concluding remarks

A comprehensive climatology of extratropical transition in the Atlantic basin has been presented. This climatology lays the foundation for further research into the factors that determine whether a specific tropical cyclone transitions. Given the extreme sparsity of data and the required resolution for accurate analyses, use of higher-resolution analyses and high-resolution numerical simulations of transition are likely to be required for detailed insight. Work in all of these areas is being pursued by the authors.

Acknowledgments. Partial support for this research came from the National Science Foundation (ATM-9508085) and NASA (NAG5-7547). The first author was funded by a Pennsylvania State University Earth System Science Center (ESSC) Graduate Fellowship and an Environmental Protection Agency (EPA) STAR Graduate Fellowship. Sincere appreciation goes out to all of these agencies for their support.

We are grateful to Jim Abraham of Environment Canada for his feedback on many of the figures presented in this paper. We thank Lixion Avila of NHC for his input on the methodology behind operational transition classification at NHC. Analyses and figures for this paper were created using the GrADS software package from COLA/IGES. Many thanks go to the folks at COLA/IGES, especially Brian Doty and Mike Fiorino, for making this software package available.

We sincerely appreciate the critical and valuable comments provided by Mike Fritsch and two anonymous reviewers.

REFERENCES

Bister, M., and K. A. Emanuel, 1998: Dissipative heating and hurricane intensity. *Meteor. Atmos. Phys.*, **65,** 233–240.

Bosart, L. F., and J. A. Bartlo, 1991: Tropical storm formation in a baroclinic environment. *Mon. Wea. Rev.*, **119,** 1979–2013.

——, and G. M. Lackmann, 1995: Postlandfall tropical cyclone reintensification in a weakly baroclinic environment: A case study of Hurricane David (September 1979). *Mon. Wea. Rev.,* **123,** 3268–3291.

Brand, S., and C. P. Guard, 1978: Extratropical storm evolution from tropical cyclones in the western North Pacific Ocean. Naval Environmental Prediction Tech. Rep. TR 78-02, 20 pp. [Available from Naval Research Laboratory/Marine Meteorology Division, 7 Grace Hopper Ave., Stop 2, Monterey, CA 93943-5502.]

DiMego, G. J., and L. F. Bosart, 1982a: The transformation of Tropical Storm Agnes into an extratropical cyclone. Part I: The observed fields and vertical motion computations. *Mon. Wea. Rev.,* **110,** 385–411.

——, and ——, 1982b: The transformation of Tropical Storm Agnes into an extratropical cyclone. Part II: Moisture, vorticity, and kinetic energy budgets. *Mon. Wea. Rev.,* **110,** 412–433.

Elsberry, R. L., Ed., 1995: Global perspectives on tropical cyclones. Rep. TD-693, WMO, Geneva, Switzerland, 289 pp.

Emanuel, K. A., 1986: An air–sea interaction theory for tropical cyclones. Part I: Steady-state maintenance. *J. Atmos. Sci.,* **43,** 585–604.

——, 1988: The maximum intensity of hurricanes. *J. Atmos. Sci.,* **45,** 1143–1155.

Gibson, J. K., P. Kållberg, S. Uppala, A. Hernandez, A. Nomura, and E. Serrano, 1997: ECMWF Re-analysis Project Report Series. Part 1: ERA description. ECMWF, Shinfield Park, Reading, United Kingdom, 72 pp.

Goldenberg, S. B., and L. J. Shapiro, 1996: Physical mechanisms for the association of El Niño and West African rainfall with Atlantic major hurricane activity. *J. Climate,* **9,** 1169–1187.

Hoskins, B. J., and P. J. Valdes, 1990: On the existence of storm-tracks. *J. Atmos. Sci.,* **47,** 1854–1864.

Jarvinen, B. R., C. J. Neumann, and M. A. S. Davis, 1984: A tropical cyclone data tape for the North Atlantic basin, 1886–1983: Contents, limitations, and uses. NOAA Tech. Memo. NWS NHC 22, NOAA/National Hurricane Center, Miami, FL, 21 pp. [Available from NOAA/Tropical Prediction Center, 11691 SW 17th St., Miami, FL 33165-2149.]

Klein, P., 1997: Extratropical transition of western North Pacific tropical cyclones. M.S. thesis, Dept. of Meteorology, Naval Postgraduate School, 101 pp. [NTIS ADA-341-420.]

Kornegay, F. C., and D. G. Vincent, 1976: Kinetic energy budget analysis during interaction of Tropical Storm Candy (1968) with an extratropical frontal system. *Mon. Wea. Rev.,* **104,** 849–859.

Landsea, C. W., 1993: A climatology of intense (or major) Atlantic hurricanes. *Mon. Wea. Rev.,* **121,** 1703–1713.

Malmquist, D., 1999: Meteorologists and Insurers Explore Extratropical Transition of Tropical Cyclones. *Eos, Trans. Amer. Geophys. Union,* **80,** 79–80.

Matano, H., and M. Sekioka, 1971: Some aspects of extratropical transformation of a tropical cyclone. *J. Meteor. Soc. Japan,* **49,** 736–743.

Molinari, J., and D. Vollaro, 1989: External influences on hurricane intensity. Part I: Outflow layer eddy angular momentum fluxes. *J. Atmos. Sci.,* **46,** 1093–1105.

——, and ——, 1990: External influences on hurricane intensity. Part II: Vertical structure and response of the hurricane vortex. *J. Atmos. Sci.,* **47,** 1902–1918.

——, S. Skubis, and D. Vollaro, 1995: External influences on hurricane intensity. Part III: Potential vorticity structure. *J. Atmos. Sci.,* **52,** 3593–3606.

Neumann, C. J., B. R. Jarvinen, C. J. McAdie, and J. D. Elms, 1993: Tropical cyclones of the North Atlantic Ocean, 1871–1992. National Climatic Data Center in cooperation with the National Hurricane Center, Coral Gables, FL, 193 pp. [Most recent track information available online at http://www.nhc.noaa.gov.]

Palmén, E., 1958: Vertical circulation and release of kinetic energy during the development of Hurricane Hazel into an extratropical storm. *Tellus,* **10,** 1–23.

Pierce, C. H., 1939: The meteorological history of the New England Hurricane of Sept. 21, 1938. *Mon. Wea. Rev.,* **67,** 237–285.

Reynolds, R. W., and T. Smith, 1995: A high-resolution global sea surface temperature climatology. *J. Climate,* **8,** 1571–1583.

Sekioka, M., 1956a: A hypothesis on complex of tropical and extratropical cyclones for typhoon in the middle latitudes. I. Synoptic structure of Typhoon Marie passing over the Japan Sea. *J. Meteor. Soc. Japan,* **34,** 276–287.

——, 1956b: A hypothesis on complex of tropical and extratropical cyclones for typhoon in the middle latitudes. II. Synoptic structure of Typhoons Louise, Kezia, and Jane passing over the Japan Sea. *J. Meteor. Soc. Japan,* **34,** 336–345.

——, 1957: A hypothesis on complex of tropical and extratropical cyclones for typhoon in the middle latitudes. III. Examples of typhoon not accompanied by extratropical cyclone in the middle latitudes. *J. Meteor. Soc. Japan,* **35,** 170–173.

Troup, A. J., 1965: The Southern Oscillation. *Quart. J. Roy. Meteor. Soc.,* **91,** 490–506.

van Loon, H., and J. C. Rogers, 1978: The seesaw in winter temperatures between Greenland and northern Europe. Part I: General description. *Mon. Wea. Rev.,* **106,** 296–310.